
High-Level Ab Initio Methods for Calculation of Potential Energy Surfaces of van der Waals Complexes

TIMOTHY J. GIESE, DARRIN M. YORK

Department of Chemistry, University of Minnesota, Minneapolis, Minnesota 55415, USA

Received 2 July 2003; accepted 15 December 2003

Published online 23 March 2004 in Wiley InterScience (www.interscience.wiley.com).

DOI 10.1002/qua.20074

ABSTRACT: A systematic series of highly correlated calculations of van der Waals potential energy surfaces (PESs) with large basis sets is presented. Reference data at the coupled-cluster theory restricted to single, double, and noniterative triple excitations [CCSD(T)] level with large singly augmented correlation-consistent basis functions, supplementary bond functions, and counterpoise corrections are provided. Results for minimum energy distances, well depths, vibrational frequencies, second virial coefficients, and Boyle temperatures are compared with corresponding experimental values. An extensive discussion of complete basis set extrapolation methods is presented. Here, the effect of extrapolation type, use of uncorrected and counterpoise-corrected PESs, and direct property extrapolation are analyzed. Last, a new multicoefficient correlation method for van der Waals potential energy surfaces (MCCM-vdW) is applied to three-body interactions of helium trimers and to $\text{He} \cdots \text{H}_2\text{O}$ interactions. Comparison with high-level CCSD(T) calculations using large basis sets demonstrates that the MCCM-vdW method is transferable to systems not considered in its parameterization. The method allows dispersion interactions of much larger systems to be studied reliably at a fraction of computational cost and offers a new tool for applications to rare-gas clusters and the development of dispersion parameters for molecular simulation force fields. © 2004 Wiley Periodicals, Inc. *Int J Quantum Chem* 98: 388–408, 2004

Key words: CCSD(T) calculations; large basis sets; multicoefficient correlation method; potential energy surfaces; van der Waals

Correspondence to: D. M. York; e-mail: york@chem.umn.edu

Contract grant sponsor: National Institutes of Health.

Contract grant number: 1R01-GM62248-01A1.

Contract grant sponsors: American Chemical Society; University of Minnesota; National Institutes of Health.

Introduction

There is a wealth of interest in research that lies at the interface of traditional disciplines of chemistry, biology, and physics. A main focus involves the integration of experimental and theoretical methods that, together, are able to paint a detailed picture of processes that span individual molecule, nanoscale and even mesoscale domains. Consequently, it is an important goal of computational chemistry to develop “multiscale” quantum models that are able to simultaneously model a broad range of spatial and temporal domains.

The role of modern computational quantum chemical techniques in this area of theoretical biophysics is manifold [1]. One particularly fruitful application of high-level quantum methods is toward the fundamental understanding of intermolecular interactions, and in the development of quantitative models that can be applied more efficiently to larger chemical systems and a greater degree of configurational space. Current-generation “molecular mechanical” force fields almost uniformly rely on quantum chemical calculations for at least part of their parameterization [2–5]. Some force fields use quantum mechanical calculations almost exclusively to determine molecular mechanical parameters. Others force fields have put forth considerable effort to adjust, in addition, a relatively small number of parameters based on bulk simulations, albeit for mixtures of only a few components [6, 7]. In addition to molecular mechanical force fields for simulations of nonreactive processes, there is great interest in the design of improved hybrid quantum mechanical/molecular mechanical (QM/MM) potentials that extend the capability of molecular simulations to reactive events [8–10]. The quantum models have to be sufficiently fast to be coupled with the extensive configurational sampling required to extract meaningful, converged free energies and other thermodynamic quantities. The inverse relation between the accuracy and computational cost of *ab initio* methods often necessitates the use of semiempirical quantum models for practical applications even with large computing resources [11]. Even more than the molecular mechanical force fields, these semiempirical QM/MM potentials must be trained against high-level *ab initio* methods to attain chemical accuracy. Consequently, the design and application of high-level quantum methods to intermo-

lecular interactions, including reactions, is of prime interest.

Often, even fairly simple interactions, such as weak dispersion forces, are particularly difficult to model quantum mechanically, requiring highly correlated theoretical levels, very large basis sets, and often special bond functions and counterpoise corrections [12, 13]. Nonetheless, the interactions are of key importance in molecular simulations of nanoscale systems (including biological macromolecules) and play major roles in the determination of hydrophobic effects, solute–solvent partition coefficients, internal pressures, and ligand binding free energies. It is interesting to note that despite their importance, the dispersion interactions are often improperly modeled, or outright neglected, in many of the most popular density functional and semiempirical quantum models applied to biological systems.

In the current paper, methods for the determination of dispersion interactions for potential energy surfaces (PESs) are discussed. The next sections provides a description of Methods, including the electronic structure methods applied in this work and the protocol used to perform complete basis-set (CBS) extrapolations and multicoefficient correlation method. The Results and Discussion section is broken down into three parts. The first subsection provides a brief survey of how well high-level quantum mechanical calculations are able to predict experimental properties related to the PESs of rare-gas dimers. The second subsection provides a detailed comparison of rare-gas dimer properties obtained from CBS extrapolations of the properties directly and derived from the CBS PESs. The third subsection discusses a new multilevel strategy for the determination of dispersion interactions of larger systems. The final section summarizes the important points of the current work and outlines future research directions toward the development of new-generation molecular mechanical and hybrid QM/MM potentials.

Methods

This section describes the computational quantum methods used in the current work, including the *ab initio* electronic structure calculations, determination of second virial coefficients, CBS limit extrapolation procedures, and multilevel fitting methods.

AB INITIO ELECTRONIC STRUCTURE CALCULATIONS

Electronic structure calculations were performed at the coupled-cluster theory restricted to single, double, and noniterative triple excitations [CSSD(T)] level of theory using the singly augmented correlation-consistent basis sets [14, 15] (aug-cc-pVTZ, aug-cc-pVQZ, aug-cc-pV5Z). The shorthand notation aTZ, aQZ, and a5Z for the basis sets is introduced and used in subsequent equations and discussion. The CCSD(T) level of theory and basis used in the current work was demonstrated previously to provide very reliable results for the weakly bound van der Waals complexes studies here [16, 17].

In many cases, the counterpoise correction scheme of Boys and Bernardi [18] was used to correct for basis set superposition error (BSSE) at a given basis set level. The calculations are denoted by the shorthand notation aTZ+CP, aQZ+CP, and a5Z+CP.

A very-high-level reference data set was constructed for certain PESs that employed the a5Z basis in addition to a supplementary set of 3s3p2d2f1g bond functions and counterpoise corrections. A detailed discussion of this reference data set is provided elsewhere [17]. These high-level reference data sets are denoted “high level” in the remainder of the text, and the basis set/counterpoise correction protocol is denoted “ref” = a5Z(3s3p2d2f1g)+CP. All electronic structure calculations were performed using the MOLPRO2000 software package [19].

COMPLETE BASIS SET EXTRAPOLATIONS

Two CBS extrapolation schemes are considered in the current work: a mixed Gaussian/exponential form (CBSI), and a single exponential form (CBSII).

In both CBS extrapolation procedures, the property of interest at a given basis-set level is modeled by a parametric form. The parameters, one of which corresponds to the property value at the CBS limit, are obtained by a nonlinear minimization procedure of a χ^2 function of the form

$$\chi^2(A^{CBS}, B^{CBS}, C^{CBS}) = \sum_{x=3}^5 (\tilde{A}(x; A^{CBS}, B^{CBS}, C^{CBS}) - A(x))^2, \quad (1)$$

where $A(x)$ is the property calculated with the basis set characterized by the “cardinal index” [20], x (i.e., $x = 3, 4, 5$ for basis sets aTZ, aQZ, and a5Z, respectively), and $\tilde{A}(x; A^{CBS}, B^{CBS}, C^{CBS})$ is the CBS model value for the same cardinal index. The parameters in the CBS model are generically denoted A^{CBS} , B^{CBS} , and C^{CBS} (see below for the specific CBSI and CBSII model forms), where A^{CBS} represents the property value at the CBS limit. In the case that the property of interest is the energy itself, it has an explicit dependence on the internuclear separation r , that is, $A^{CBS} = E^{CBS}(r)$. A complete knowledge of $E^{CBS}(r)$ forms a PES, from which other important properties can be derived, such as the minimum energy internuclear distance (R_e), binding energy well depth (D_e), vibrational frequency (ω_e) and force constant (k_e), and second virial coefficient ($B_2(T)$). Hence, there are two ways one can estimate the values of such properties at the CBS limit: by direct CBS extrapolation via minimization of Eq. (1) with respect to the parameters A^{CBS} , B^{CBS} , and C^{CBS} (the optimized value of A^{CBS} providing the CBS limit value), or by derivation from the CBS potential energy curve $E^{CBS}(r)$. To distinguish the CBS property values determined from these two procedures, the values of the latter, (i.e., the value derived from the CBS potential energy curve $E^{CBS}(r)$), is henceforth superscripted with an asterisk (e.g., A^{CBS*}).

The mixed Gaussian/exponential scheme used here, denoted CBSI, was first suggested by Woon and Dunning [21] and Peterson et al. [22] and has the form

$$\tilde{A}(x) = A^{CBSI} + B^{CBSI}e^{-(x-1)} + C^{CBSI}e^{-(x-1)^2}, \quad (2)$$

where A^{CBSI} is the CBS limit value estimated from the CBSI extrapolation scheme and, as mentioned above, the index x corresponds to the cardinal index [20] of the basis. The same property A , if derived from the CBS potential energy curve $E^{CBSI}(r)$, would be designated A^{CBSI*} .

The second type of CBS extrapolation procedure considered, CBSII, is the exponential form proposed by Feller [23, 24] and Feller and Peterson [25] and subsequently tested against rare-gas systems using counterpoise- and un-counterpoise-corrected energies [26],

$$\tilde{A}(x) = A^{CBSII} + B^{CBSII}e^{-C^{CBSII}x}. \quad (3)$$

As before, x is the “cardinal index” of the basis, A^{CBSII} is the estimated CBS limit value for property

A , and B^{CBSII} and C^{CBSII} are parameters determined through the optimization of Eq. (1).

All CBS extrapolations used the series of basis sets aTZ, aQZ, and a5Z.

CONSTRUCTION OF CBS-EXTRAPOLATED POTENTIAL ENERGY SURFACES

The calculation of the CBS-extrapolated binding energy surfaces was performed in the following manner:

$$E_b^{CBS}(A : B; r_{AB}) = E^{CBS}(A : B; r_{AB}) - E^{CBS}(A + B; r_{AB}), \quad (4)$$

where $E^{CBS}(A : B; r_{AB})$ is the CBS-extrapolated total energy of the dimer AB at a separation r_{AB} , and $E^{CBS}(A + B; r_{AB})$ is the CBS extrapolated sum of the monomer energies, which, in the case of counterpoise corrections, may also depend on r_{AB} (in the case of un-counterpoise-corrected monomer energies, there is no r_{AB} dependence).

The CBS extrapolation procedure of the PES requires extrapolations of two total energies. This approach was chosen over the single extrapolation of the binding energy directly. The total energy convergence of the monomers and dimer is exponentiallike in the series of aTZ through a5Z for both the counterpoise-corrected and -uncorrected values throughout the PES. In contrast, the binding energies in the series of aTZ through a5Z do not appear to converge in an exponentiallike fashion for all internuclear separations. As discussed further in the following sections, the counterpoise-corrected binding energy surfaces converge more systematically for most values of r_{AB} than do the uncorrected binding energies.

MULTICOEFFICIENT CORRELATION METHOD FOR van der WAALS COMPLEXES

The theoretical levels Hartree–Fock (HF), second-order Møller–Plesset (MP2), CCSD, and CCSD(T) form a systematic hierarchy based on the HF single determinant, and in most electronic structure packages, calculation at any of these levels requires prior calculations at all of the lower levels. Consequently, the energies at lower theoretical levels in this series are typically available at no extra computational cost. However, the scaling of the computational effort of the higher levels of theory precludes their application to systems with a very

large number of particles and/or basis functions. It is the objective of a multicoefficient correlation method (MCCM) to exploit the additivity of basis set and treatment of electron correlation to construct a quantum energy model that is a linear combination of theory/basis set levels such that use of a highly correlated method is never required at a high basis set level.

The MCCM used here is the multicoefficient correlation method–van der Waals (MCCM–vdW) of Giese and York [27]. The MCCM–vdW model was designed to reproduce the weak dispersion interactions of rare-gas dimer PESs as calculated at the high-level reference protocol described above. The MCCM–vdW model is constructed as the sum of two energy components:—HF-SCF energy and correlation energy—denoted MCCM–vdW(X) and MCCM–vdW(C), respectively. The form of the MCCM–vdW energy components are given by:

$$E^{MCCM-vdW} = a_1 E^{HF/aDZ} + a_2 E^{MP2/aDZ} + a_3 E^{CCSD/aDZ} + a_4 E^{CCSD(T)/aDZ} + a_5 E^{HF/aTZ} + a_6 E^{MP2/aTZ} + a_7 E^{CCSD/aTZ} + a_8 E^{HF/aQZ} + a_9 E^{MP2/aQZ} + a_{10} E^{HF/a5Z}. \quad (5)$$

The total energy can be decomposed into a Hartree–Fock self-consistent field (HF-SCF) energy term, E_{HF} , and a correlation energy term, E_C ; that is, $E = E_{HF} + E_C$, where E_{HF} and E_C , within the MCCM–vdW model, are given by

$$E_{HF}^{MCCM-vdW} = (a_1 + a_2 + a_3 + a_4) E^{HF/aDZ} + (a_5 + a_6 + a_7) E^{HF/aTZ} + (a_8 + a_9) E^{HF/aQZ} + a_{10} E^{HF/a5Z} \quad (6)$$

and

$$E_C^{MCCM-vdW} = a_2 (E^{MP2/aDZ} - E^{HF/aDZ}) + a_3 (E^{CCSD/aDZ} - E^{HF/aDZ}) + a_4 (E^{CCSD(T)/aDZ} - E^{HF/aDZ}) + a_6 (E^{MP2/aTZ} - E^{HF/aTZ}) + a_7 (E^{CCSD/aTZ} - E^{HF/aTZ}) + a_9 (E^{MP2/aQZ} - E^{HF/aQZ}). \quad (7)$$

The MCCM–vdW model was demonstrated to accurately reproduce the interaction, HF-SCF, and correlation components of the energy for rare-gas dimers and trimers, rare-gas trimer three-body, and rare-gas water energies [27]. This MCCM–vdW is novel in that it provides individual components of

the energy and thus could be applied directly to the determination of dispersion terms in new-generation molecular mechanical force field models. The protocol of fitting simultaneously to the total energy and individual HF-SCF and correlation components was observed to produce a more transferable and, overall, more reliable model. A detailed discussion of and applications with MCCM-vdW are found in Ref. [27].

Results and Discussion

Dispersion (van der Waals) interactions between rare-gas atoms have been studied extensively with ab initio methods [16, 28–34]. Accurate calculations of dispersion interactions [12, 13, 35] require high-level quantum models and very large basis sets (with careful attention paid to BSSEs [36]) to achieve both convergence and high accuracy. Calculations at the CCSD(T) level of theory using a large augmented correlation consistent basis (aug-cc-pV5Z) [33, 37] supplemented with a set of (3s3p2d2f1g) bond functions [38–40] and using a counterpoise correction scheme [18, 41] lead to excellent agreement with the experimental binding curves of Ogilvie and Wang [42, 43] in the region around the binding minima [16, 17].

The understanding of the nature of intermolecular (or interatomic) dispersion interactions is critical to the development of new-generation molecular simulation force fields. The current work focuses on the calculation of accurate binding PESs and properties derived therefrom, for rare-gas interactions, including interactions with polar molecules. There are three main subsections. The first subsection addresses the question: How well can high-level ab initio calculations reproduce known properties derivable from the two-body PES? There has been an abundance of work in this area, and it is the purpose here to compare results of very high-level calculations with experiment (convergence behavior and other technical details are discussed extensively elsewhere). The second subsection delves into the problem of deriving accurate PESs and related properties in the complete basis set limit using different CBS extrapolation procedures and counterpoise corrections. The final subsection outlines a recently developed MCCM for van der Waals interactions that is considerably more efficient for larger systems than CCSD(T) methods with comparably accurate basis sets. The method does not require counterpoise corrections and may

be used as a practical tool to obtain accurate data for parameterization of dispersion terms in molecular simulation force fields.

ACCURATE PROPERTIES OF THE TWO-BODY PES

Table I compares the calculated and experimental equilibrium distance (R_e), well depth (D_e), vibrational frequency (ω_e), and force constant (k_e), in addition to the classical and quantum corrected second virial coefficient [$B_2(T = 300\text{K})$] and Boyle temperature (T_B) (see below for further details). The calculated results agree closely with experimental values. The largest error for R_e , D_e , and ω_e is 0.022 Å (Ar–Ar), 0.008 kcal/mol (Ar–Ar), and 0.9 cm^{-1} (He–Ne/He–Ar), respectively. The values are well within an acceptable error margins for typical molecular simulation force fields.

Virial coefficients are derived from the virial equation of state in the grand canonical ensemble and are used to expand the pressure p as a power series in the density ρ [44]:

$$\frac{p}{k_B T} = \rho + B_2(T)\rho^2 + B_3(T)\rho^3 \dots, \quad (8)$$

where k_B is the Boltzmann constant, T is the absolute temperature, and $B_j(T)$ is the j^{th} virial coefficient. The second virial coefficient, $B_2(T)$, is a property of the two-body interaction and is a focus of the current discussion. In the classical limit, the second virial coefficient for an n -component mixture of monatomic gas particles can be calculated as

$$B_2(T) = \sum_{i=1}^n \sum_{j=1}^n B_{ij}(T) x_i x_j, \quad (9)$$

where x_i is the mole fraction of component i and $B_{ij}(T)$ is defined by

$$B_{ij}(T) = -\frac{1}{2} \int_0^\infty f_{ij}(r; T) 4\pi r^2 dr + B_{ij}^{\text{QC}}(T), \quad (10)$$

where $f_{ij}(r; T)$ is the Mayer f -function for the ij particle pair, defined as

$$f_{ij}(r; T) = e^{-V_{ij}(r)/k_B T} - 1 \quad (11)$$

TABLE I
Comparison of the calculated (bold) and experimental (*italics*) binding energy curves for rare-gas dimers.^a

Dimer	R_e	D_e	ω_e	k_e	$B_2^C(T)$	T_B^C	$B_2^{QMC}(T)$	T_B^{QMC}
He-He	2.977	0.021	32.7	0.183	11.64	—	12.20	—
	<i>2.970</i>	<i>0.022</i>	<i>33.1</i>	<i>0.187</i>	<i>11.77</i>	—	<i>11.77</i>	—
Ne-Ne	3.099	0.082	29.0	0.727	11.73	112.41	11.93	109.60
	<i>3.091</i>	<i>0.084</i>	<i>28.4</i>	<i>0.696</i>	<i>11.16</i>	<i>115.4</i>	<i>11.16</i>	<i>115.4</i>
Ar-Ar	3.779	0.277	30.3	1.562	-13.61	396.14	-13.37	394.70
	<i>3.757</i>	<i>0.285</i>	<i>30.8</i>	<i>1.622</i>	<i>-16.40</i>	<i>416.49</i>	<i>-16.40</i>	<i>416.49</i>
He-Ne	3.030	0.042	35.7	0.364	12.10	81.32	12.51	68.63
	<i>3.031</i>	<i>0.041</i>	<i>34.8</i>	<i>0.346</i>	<i>12.07</i>	<i>77.82</i>	<i>12.07</i>	<i>77.82</i>
He-Ar	3.494	0.059	35.6	0.393	8.78	202.58	9.24	198.73
	<i>3.480</i>	<i>0.057</i>	<i>34.7</i>	<i>0.374</i>	<i>7.51</i>	<i>307.57</i>	<i>7.51</i>	<i>207.57</i>
Ne-Ar	3.495	0.129	27.3	0.857	5.28	248.04	5.50	245.39
	<i>3.489</i>	<i>0.134</i>	<i>28.1</i>	<i>0.903</i>	<i>4.38</i>	<i>256.43</i>	<i>4.38</i>	<i>256.43</i>

^a Comparison of calculated and experimental values for the equilibrium (minimum energy) distance R_e (Å), dissociation energy D_e (kcal/mol), vibrational wave number ω_e (cm^{-1}), force constant k_e ($\text{kcal/mol} \cdot \text{Å}^2$), the second virial coefficients at 300K $B_2(T)$ (cm^3/mol), and Boyle temperature T_B (K). For the virial coefficients and Boyle temperatures, results derived from the classical virial formula (superscripted "Cl") and including quantum corrections (superscripted "QMC") are shown. See text for additional details. Experimental values for R_e , D_e , ω_e , and k_e were taken from Ogilvie and Wang for homodimers [42] and heterodimers [43]. Experimental values for $B_2(T)$ and T_B were taken from the reference data of Kestin et al. [45].

and $V_{ij}(r)$ is the classical Born–Oppenheimer two-body pair potential between particles i and j . In Eq. (10), $B_{ij}^{QC}(T)$ is a quantum correction to the classical second virial coefficient. Quantum corrections, most important for very light particles at low temperatures, can be derived by expansion of the canonical partition function in a power series in Planck's constant h [44]. Only the h^2 term is considered here in the expression for $B_{ij}^{QC}(T)$:

$$B_{ij}^{QC}(T) = \frac{h^2}{24\pi\mu_{ij}(kT)^3} \int_0^\infty e^{-\beta V_{ij}(r)} \left(\frac{dV_{ij}(r)}{dr} \right)^2 r^2 dr, \quad (12)$$

where μ_{ij} is the reduced mass of atoms i and j . The Boyle temperature (T_B) for a gaseous mixture is defined as the temperature for which the second virial coefficient vanishes, and it is a quantity easily measured experimentally.

In the current work, the two-body pair potentials $V_{ij}(r)$ calculated from high-level electronic structure calculations and fit to analytic forms are used to calculate the second virial coefficients $B_2(T)$ and Boyle temperatures T_B for rare gas mixtures according to Eqs. (9–12). Table I compares the calculated classical and quantum corrected second virial coefficients at 300 K and Boyle temperatures with ex-

perimental values [45], and Figure 1 compares the classical and quantum corrected second virial coefficients with experimental values. Overall, the agreement between the theoretical and experimental second virials is reasonably close. The theoretical curves at this theory/basis level slightly overestimate the experimental $B_2(T = 300)$ values. Inclusion of quantum corrections (to second order) results in worse agreement between experimental and calculated values. The mean signed error across all the dimers is 0.91 and 1.26 cm^3/mol for classical and quantum-corrected values, respectively, the largest error occurring with Ar–Ar (2.79 and 3.03 cm^3/mol) for classical and quantum-corrected values, respectively. The errors in the second virial coefficients can be explained though an overall slight underbinding of the calculated rare-gas dimers that becomes magnified with inclusion of zero-point energy corrections.

The theoretical $B_2(T)$ curves at this theory/basis level slightly overestimate the experimental values (Fig. 1), with the largest errors occurring for He–He at very low temperatures, where quantum corrections are expected to be quite large. The He–He van der Waals potential is notoriously difficult and has been the topic of numerous investigations [36, 40–56]. It is the purpose here to assess how well a high-level ab initio PES can reproduce experimental

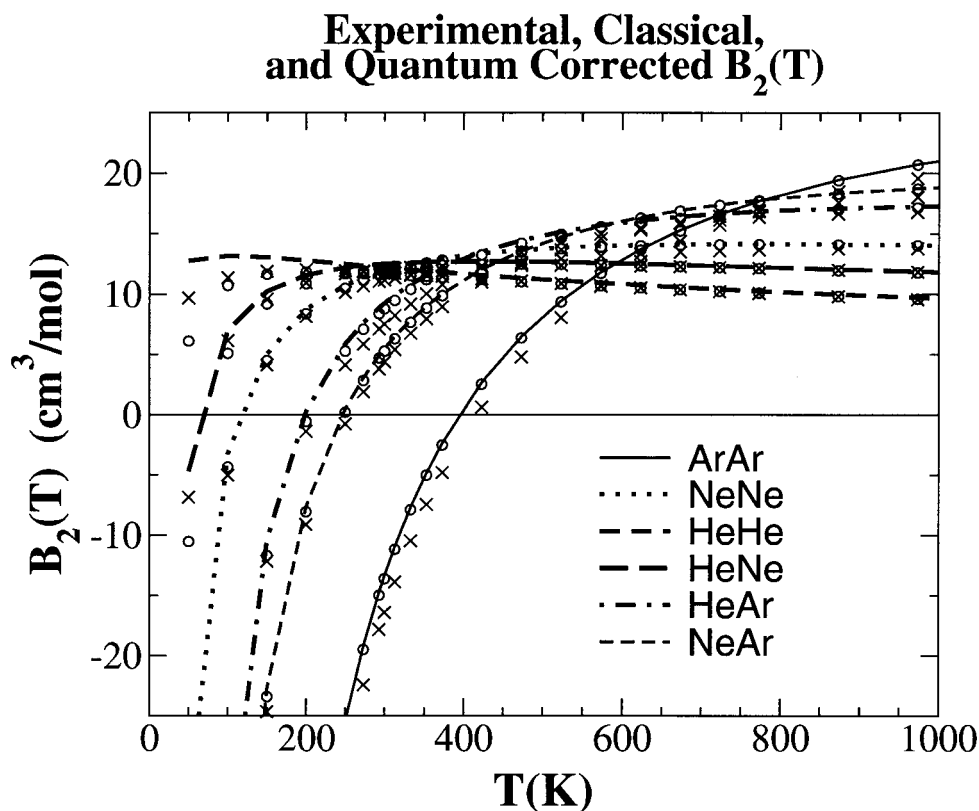


FIGURE 1. Comparison of classical, quantum-corrected, and experimental second virial coefficients using the high-level reference data (see text). Open circles (\circ) indicate classical second virial data and lines mark quantum corrected virial data. Exes (\times) indicate experimental values as reported in Ref. [45]. For complimentary discussion of rare gas second virial coefficients, see Refs. [90–92].

second virial coefficients without recourse into empirical adjustment [57]. The overall percent error for T_B with quantum corrections is around 4–5%, with the exception of He–Ne (11.8%), the lightest dimer with the lowest Boyle temperature that could be compared.

CBS EXTRAPOLATIONS

A large amount of attention has been spent on the prediction of properties in the limit of a CBS based on extrapolation procedures [21–26, 54, 58–80], including studies with particular emphasis on the prediction of equilibrium geometries [26, 62, 69, 76, 77, 80]. Specifically, comparisons have been made between CBS extrapolations of geometrical parameters, that is, bond lengths, as observed from PESs calculated with and without counterpoise correction. It was demonstrated in several studies that the convergence behavior of geometrical parameters as observed on coun-

terpoise-corrected surfaces is more systematic than those observed on uncorrected surfaces [26, 77, 80], whereas other work suggested that the difference in CBS extrapolated properties are very similar with respect to accounting for BSSE through counterpoise corrections [62, 64].

Relatively little attention has been spent on the extrapolation of entire PESs [81], which have the most relevance for applications to reaction dynamics and the design of new-generation quantum models for molecular simulations. It is not obvious that a CBS extrapolated PES leads to the same geometrical properties as those properties extrapolated directly. In this section, comparisons are made between the properties derived from CBS extrapolated rare-gas PESs and those obtained through direct CBS extrapolation, both of which comprise inherently different procedures. Moreover, comparisons are made for two different CBS extrapolation types (designated CBSI and CBSII; see Methods)

TABLE II

Comparison of He₂ CCSD(T)/CBS extrapolated properties with high-level reference calculations and those of Ogilvie.

Basis ^a	CP ^b	R_e	$\Delta_{R_e}^{OW}$	$\Delta_{R_e}^{HL}$	$D_e \times 10^5$	$\Delta_{D_e}^{OW}$	$\Delta_{D_e}^{HL}$	$\omega_e \times 10^4$	$\Delta_{\omega_e}^{OW}$	$\Delta_{\omega_e}^{HL}$
aTZ		5.7019	-1.59	-1.35	3.1330	9.82	6.99	1.3360	11.46	10.46
aQZ		5.6473	-0.61	-0.38	3.2144	7.47	4.57	1.4266	5.46	4.39
a5Z		5.6514	-0.69	-0.45	3.2520	6.39	3.45	1.3981	7.34	6.29
aTZ	x	5.7513	-2.47	-2.23	2.7113	21.96	19.51	1.2822	15.02	14.06
aQZ	x	5.6946	-1.46	-1.22	2.9654	14.64	11.96	1.4377	4.72	3.64
a5Z	x	5.6600	-0.84	-0.60	3.1246	10.06	7.24	1.3961	7.48	6.43
CBSII		5.6488	-0.64	-0.40	3.2844	5.46	2.49	1.4154	6.20	5.14
CBSI		5.6564	-0.78	-0.54	3.2740	5.76	2.80	1.3809	8.48	7.45
CBSII	x	5.6053	0.13	0.37	3.5060	-0.92	-4.09	1.4238	5.64	4.57
CBSI	x	5.6397	-0.48	-0.24	3.2179	7.37	4.47	1.3708	9.15	8.12
CBSII*		5.6729	-1.07	-0.83	3.2788	5.61	2.66	1.3338	11.61	10.61
CBSI*		5.6536	-0.73	-0.49	3.2729	5.79	2.83	1.3553	10.19	9.17
CBSII*	x	5.6256	-0.23	0.01	3.2697	5.88	2.93	1.3599	9.88	8.86
CBSI*	x	5.6364	-0.42	-0.18	3.2212	7.28	4.37	1.3456	10.83	9.81
OW	NA	5.6128	0.00	0.24	3.4740	0.00	-3.14	1.5090	0.00	-1.13
HL	x	5.6260	-0.24	0.00	3.3684	3.04	0.00	1.4920	1.12	0.00

All values are in atomic units.

^a Abbreviation "HL" refers to the high-level calculations as described in the text; "OW" refers to the data of Ogilvie [42]. The columns $\Delta_{Property}^{Ref}$ are the relative signed difference (see text) of the property as compared with Ogilvie and the high-level calculations.^b Abbreviation "x" denotes the use of counterpoise correction or the use of counterpoise corrected data in the CBS extrapolation. The use of counterpoise correction does not apply to the data of Ogilvie.

using both uncorrected and counterpoise-corrected rare-gas data. The distinction between procedure and type is important because the work focuses on the comparison of procedures. The purpose of examining more than one type is to address the concern that the results may be spuriously associated with the type of extrapolation used. Although there are a variety of extrapolation types available [25, 81, 82], CBSI and CBSII are commonly used extrapolation types found in the literature and are henceforth used here.

This subsection is further broken down into discussions regarding: convergence of dimer properties with respect to basis and use of counterpoise correction, comparison of dimer properties with respect to CBS procedure (direct CBS extrapolation of the property versus calculation from the CBS extrapolated PESs), and analysis of errors across all dimers for each extrapolation type of each procedure with and without counterpoise-corrected data.

Convergence Behavior of Dimer Properties

It is now recognized [26, 77, 80] that the convergence of properties derived from PESs without the

use of counterpoise correction are not systematic in many cases and that the convergence behavior of properties should be evaluated on a case-by-case basis [24].

Tables II–VII compare the experimental and calculated CCSD(T) values of R_e , D_e , and ω_e using different basis sets, counterpoise correction schemes, and CBS extrapolations. Of particular interest in this section are the uncorrected and counterpoise-corrected properties with the aTZ, aQZ, and a5Z basis sets. The properties are compared with two sets of reference values: the experimentally derived values of Ogilvie and Wang (designated "OW") [42, 83] and calculated from the high-level reference protocol described earlier in the Methods section (designated "HL"). Comparisons are made through a signed relative difference

$$\Delta_A^{Ref} = \frac{A^{Ref} - \bar{A}}{|A^{Ref}|} \times 100, \quad (13)$$

where A^{Ref} is the property derived from the reference potential (Ref = OW or HL) and \bar{A} is the corresponding property calculated at the CCSD(T)

TABLE III
Comparison of Ne₂ CCSD(T)/CBS extrapolated properties with high-level reference calculations and those of Ogilvie.

Basis ^a	CP ^b	R_e	$\Delta_{R_e}^{OW}$	$\Delta_{R_e}^{HL}$	$D_e \times 10^4$	$\Delta_{D_e}^{OW}$	$\Delta_{D_e}^{HL}$	$\omega_e \times 10^4$	$\Delta_{\omega_e}^{OW}$	$\Delta_{\omega_e}^{HL}$
aTZ		5.8757	-0.57	-0.32	1.7194	-28.51	-31.82	1.4839	-14.45	-12.11
aQZ		5.8496	-0.12	0.12	1.5160	-13.30	-16.22	1.2114	6.57	8.48
a5Z		5.8618	-0.33	-0.09	1.3746	-2.73	-5.38	1.3117	-1.16	0.90
aTZ	x	6.0838	-4.13	-3.88	0.8162	39.00	37.43	1.0339	20.26	21.89
aQZ	x	5.9577	-1.97	-1.72	1.0582	20.91	18.87	1.1694	9.81	11.65
a5Z	x	5.9060	-1.09	-0.84	1.1765	12.07	9.80	1.1369	12.32	14.11
CBSII		5.8624	-0.34	-0.09	1.0587	20.87	18.83	1.3357	-3.01	-0.91
CBSI		5.8694	-0.46	-0.22	1.2915	3.47	0.98	1.3722	-5.83	-3.67
CBSII	x	5.8702	-0.47	-0.23	1.3349	0.23	-2.34	1.1586	10.64	12.47
CBSI	x	5.8759	-0.57	-0.33	1.2457	6.90	4.50	1.1171	13.85	15.60
CBSII*		5.8791	-0.63	-0.38	1.2383	7.45	5.07	1.5165	-16.96	-14.57
CBSI*		5.8675	-0.43	-0.18	1.2917	3.46	0.97	1.3687	-5.56	-3.40
CBSII*	x	5.8735	-0.53	-0.29	1.2673	5.28	2.84	1.2660	2.36	4.35
CBSI*	x	5.8814	-0.66	-0.42	1.2494	6.62	4.21	1.2973	-0.06	1.99
OW	NA	5.8425	0.00	0.24	1.3380	0.00	-2.58	1.2966	0.00	2.04
HL	x	5.8568	-0.24	0.00	1.3044	2.51	0.00	1.3236	-2.08	0.00

All values are in atomic units.

^a Abbreviation "HL" refers to the high-level calculations as described in the text; "OW" refers to the data of Ogilvie [42]. The columns $\Delta_{Property}^{Ref}$ are the relative signed difference (see text) of the property as compared with Ogilvie and the high-level calculations.

^b Abbreviation "x" denotes the use of counterpoise correction or the use of counterpoise corrected data in the CBS extrapolation. The use of counterpoise correction does not apply to the data of Ogilvie.

level at a particular basis set/counterpoise correction scheme or CBS extrapolation. Properties derived from the CBS-extrapolated PES are marked with an asterisk, whereas those obtained from direct CBS extrapolation are unmarked; however, a discussion of the CBS extrapolations are deferred to in the next section.

Of the properties derived from raw PESs, for example, aTZ, aQZ, and a5Z, without counterpoise correction, more than half do not monotonically converge but instead exhibit oscillatory behavior. A specific example of the nonmonotonic behavior is the D_e values for HeAr: the a5Z value (9.92×10^{-2} mE_h) is nearly the same as the aTZ value (9.90×10^{-2} mE_h) but significantly different from the aQZ value (9.67×10^{-2} mE_h). Also of concern are instances in which the difference in property values between aTZ and aQZ are less than the difference between aQZ and a5Z. An example of this behavior can be seen with R_e from the uncorrected surfaces of HeAr.

These and other examples apparent in the tables justify considerably skepticism with regard to direct extrapolation of properties calculated from un-

corrected PESs to the CBS limit. In the examples provided, it appears as though the values are either divergent or converge in a form that the monotonic behavior of many extrapolation procedures cannot accommodate. The observed convergence behavior of properties derived from PESs without counterpoise correction are in agreement with the observations of others [26], to whom the reader is referred for a detailed study. Of interest in the following sections are the extrapolation of PESs from which the properties can be calculated. Unlike the values of the properties, the dimer and sum of the monomer total energies do converge systematically and monotonically with increasing basis both with and without the use of counterpoise correction.

In contrast, the counterpoise-corrected PESs generally result in properties that converge monotonically; however, one exception is ω_e of He₂. There are instances in which it appears that the counterpoise-corrected values converge much more slowly and sometimes even from the opposite direction of the uncorrected values. An example is the D_e values of NeAr: the uncorrected values converge from above as 0.2274 (aTZ) to 0.2176 mE_h (a5Z), whereas the

TABLE IV

Comparison of Ar₂ CCSD(T)/CBS extrapolated properties with high-level reference calculations and those of Ogilvie.

Basis ^a	CP ^b	R_e	$\Delta_{R_e}^{OW}$	$\Delta_{R_e}^{HL}$	$D_e \times 10^4$	$\Delta_{D_e}^{OW}$	$\Delta_{D_e}^{HL}$	$\omega_e \times 10^4$	$\Delta_{\omega_e}^{OW}$	$\Delta_{\omega_e}^{HL}$
aTZ		7.2100	-1.54	-0.97	4.3357	4.41	1.87	1.3975	0.66	-1.38
aQZ		7.1872	-1.22	-0.65	4.3644	3.77	1.22	1.3421	4.60	2.64
a5Z		7.1434	-0.61	-0.03	4.6010	-1.44	-4.14	1.3319	5.33	3.38
aTZ	x	7.3622	-3.69	-3.10	3.2512	28.32	26.41	1.1569	17.76	16.08
aQZ	x	7.2339	-1.88	-1.30	3.7880	16.48	14.26	1.1952	15.04	13.30
a5Z	x	7.1824	-1.16	-0.58	4.1358	8.82	6.39	1.3329	5.25	3.31
CBSII		7.0918	0.12	0.69	4.8128	-6.11	-8.93	1.3295	5.49	3.55
CBSI		7.1176	-0.24	0.33	4.7411	-4.53	-7.31	1.3260	5.74	3.81
CBSII	x	7.1480	-0.67	-0.10	4.5856	-1.10	-3.79	1.4198	-0.92	-2.99
CBSI	x	7.1524	-0.73	-0.16	4.3398	4.32	1.78	1.4143	-0.54	-2.60
CBSII*		7.1068	-0.09	0.48	4.8812	-7.62	-10.48	1.5241	-8.34	-10.56
CBSI*		7.1209	-0.29	0.28	4.7491	-4.71	-7.49	1.5128	-7.54	-9.74
CBSII*	x	7.1495	-0.69	-0.12	4.4128	2.71	0.12	1.3291	5.52	3.58
CBSI*	x	7.1512	-0.71	-0.14	4.3466	4.17	1.62	1.3163	6.43	4.52
OW	NA	7.1004	0.00	0.57	4.5356	0.00	-2.66	1.4068	0.00	-2.05
HL	x	7.1411	-0.57	0.00	4.4183	2.59	0.00	1.3785	2.01	0.00

All values are in atomic units.

^a Abbreviation "HL" refers to the high-level calculations as described in the text; "OW" refers to the data of Ogilvie [42]. The columns $\Delta_{Property}^{Ref}$ are the relative signed difference (see text) of the property as compared with Ogilvie and the high-level calculations.

^b Abbreviation "x" denotes the use of counterpoise correction or the use of counterpoise corrected data in the CBS extrapolation. The use of counterpoise correction does not apply to the data of Ogilvie.

counterpoise-corrected values converge below from 0.1279 (aTZ+CP) to 0.1890 mE_h (a5Z+CP). Although the counterpoise-corrected values converge smoothly, they are further away from the CBS limit.

As suggested by others, one should apply CBS extrapolations upon assessment of the data on a case-by-case basis [24]. Two common difficulties may arise in assessing a series of BSSE-tainted properties for application to CBS extrapolations: (1) nonmonotonic convergence of uncorrected data may be observed, suggesting that counterpoise-corrected data might be more appropriate for use in CBS extrapolation; (2) counterpoise-corrected data, especially with smaller basis sets, may be sufficiently far from the CBS limit as to be of questionable reliability for use in CBS extrapolation. In cases where CBS extrapolation is suspect, there is no clear-cut general solution, and, hence, care should be taken to derive the most reliable solution, which may not necessarily be the value derived from the largest affordable basis set. For example, consider the D_e values of HeAr described earlier. Although the values of aTZ and a5Z are close, the value that

agrees best with that of Ogilvie is aTZ. In comparison with the high-level reference data, the value that agrees best is aQZ.

Comparison between Extrapolated Properties and Extrapolated Potential Energy Surfaces

In this section, Tables II–VII are further examined. The focus is shifted away from the raw data (e.g., aTZ, aTZ+CP, aQZ, etc.) and is instead concentrated on the CBS extrapolation procedures. The following CBS extrapolation procedures are compared: (1) direct extrapolation of properties using the CBSI and CBSII types (designated CBSI and CBSII, respectively); and (2) derivation of properties from the extrapolated PES using the CBSI and CBSII types (designated CBSI* and CBSII*, respectively). To avoid confusion, CBSI and CBSII are referred to as extrapolation types, as opposed to extrapolation procedures or extrapolation methods.

Illustrated in Figures 2 and 3 are the respective uncorrected and counterpoise-corrected CBSI and CBSII extrapolated PESs of Ar₂. For comparison, the binding PESs related to the total energy surfaces

TABLE V

Comparison of HeNe CCSD(T)/CBS extrapolated properties with high-level reference calculations and those of Ogilvie.

Basis ^a	CP ^b	R_e	$\Delta_{R_e}^{OW}$	$\Delta_{R_e}^{HL}$	$D_e \times 10^5$	$\Delta_{D_e}^{OW}$	$\Delta_{D_e}^{HL}$	$\omega_e \times 10^4$	$\Delta_{\omega_e}^{OW}$	$\Delta_{\omega_e}^{HL}$
aTZ		5.7337	-0.08	-0.15	8.9247	-36.18	-34.02	1.7530	-10.31	-7.76
aQZ		5.6991	0.52	0.46	7.7140	-17.70	-15.84	1.6172	-1.77	0.59
a5Z		5.7237	0.09	0.03	6.9510	-6.06	-4.38	1.5122	4.84	7.04
aTZ	x	5.9012	-3.01	-3.07	4.7092	28.15	29.28	1.4222	10.50	12.58
aQZ	x	5.8105	-1.42	-1.49	5.6021	14.52	15.88	1.5849	0.26	2.57
a5Z	x	5.7681	-0.68	-0.75	6.0855	7.15	8.62	1.5273	3.89	6.11
CBSII		5.7259	0.05	-0.01	5.1308	21.71	22.95	1.2932	18.62	20.50
CBSI		5.7384	-0.17	-0.23	6.5034	0.77	2.34	1.4505	8.72	10.84
CBSII	x	5.7310	-0.04	-0.10	7.3671	-12.41	-10.63	1.5615	1.74	4.01
CBSI	x	5.7434	-0.25	-0.31	6.3685	2.83	4.37	1.4925	6.08	8.25
CBSII*		5.7074	0.38	0.31	6.7024	-2.27	-0.65	1.6141	-1.57	0.78
CBSI*		5.7376	-0.15	-0.21	6.5108	0.66	2.23	1.5953	-0.39	1.94
CBSII*	x	5.7567	-0.49	-0.55	6.2541	4.57	6.09	1.5958	-0.42	1.90
CBSI*	x	5.7401	-0.20	-0.26	6.3816	2.63	4.17	1.4925	6.08	8.26
OW	NA	5.7289	0.00	-0.06	6.5539	0.00	1.58	1.5891	0.00	2.31
HL	x	5.7254	0.06	0.00	6.6594	-1.61	0.00	1.6268	-2.37	0.00

All values are in atomic units.

^a Abbreviation "HL" refers to the high-level calculations as described in the text; "OW" refers to the data of Ogilvie [83]. The columns $\Delta_{Property}^{Ref}$ are the relative signed difference (see text) of the property as compared with Ogilvie and the high-level calculations.

^b Abbreviation "x" denotes the use of counterpoise correction or the use of counterpoise corrected data in the CBS extrapolation. The use of counterpoise correction does not apply to the data of Ogilvie.

used in the extrapolation procedure, the high-level reference potential, and the potential of Ogilvie and Wang [42] are included. The counterpoise-corrected CBSII PES is nearly indistinguishable from the high-level reference potential. In comparing the counterpoise-corrected versus uncorrected extrapolated PESs, the uncorrected surfaces are more bound than both reference potentials.

An important result from the tabulated data is that the two extrapolation procedures can result in significantly different values. An example of significantly different results are those obtained for ω_e of He₂. Significant differences can be found between the extrapolation procedures for both extrapolation types with and without counterpoise-corrected data; however, counterpoise-corrected CBSI and CBSI* show the greatest stability. One possible explanation for the large differences is the oscillatory behavior of the ab initio data, as discussed in the previous section, for the direct extrapolation of properties. Oscillatory behavior is not observed in the total energies of Eq. (4). One may think that the oscillatory behavior makes a direct extrapolation less reliable; however, in several instances, the di-

rect property extrapolations compare better with both the reference values than those derived from the CBS-extrapolated PES. In fact, the uncorrected aTZ value of ω_e compares better with the reference data than with CBSII*.

To further support the above point, the ω_e values of Ar₂ are considered. The major difference between the raw ω_e values of He₂ and Ar₂ is the convergence behavior. With respect to basis (for both counterpoise corrected and uncorrected), He₂ displays oscillating value of ω_e , whereas those of Ar₂ converge monotonically. Therefore, part of the discussion is to further examine the possible explanation for the large differences as given in the previous paragraph. Let it be said that the Ar₂ counterpoise-corrected values are better described as diverging rather than converging with respect to the cardinal indices considered. Although the property agrees more with the expected value with increasing basis, the change occurs more rapidly in moving from the cardinal indices 4 to 5 than for 3 to 4. Even without the oscillatory behavior, direct extrapolations of the properties produce values that agree much better with both reference values than

TABLE VI
Comparison of HeAr CCSD(T)/CBS extrapolated properties with high-level reference calculations and those of Ogilvie.

Basis ^a	CP ^b	R_e	$\Delta_{R_e}^{OW}$	$\Delta_{R_e}^{HL}$	$D_e \times 10^5$	$\Delta_{D_e}^{OW}$	$\Delta_{D_e}^{HL}$	$\omega_e \times 10^4$	$\Delta_{\omega_e}^{OW}$	$\Delta_{\omega_e}^{HL}$
aTZ		6.6278	-0.75	-0.38	9.9174	-8.27	-5.33	1.5437	2.46	4.77
aQZ		6.6261	-0.72	-0.36	9.6711	-5.58	-2.71	1.6343	-3.27	-0.82
a5Z		6.5977	-0.29	0.07	9.9003	-8.08	-5.15	1.6065	-1.51	0.89
aTZ	x	6.7926	-3.25	-2.88	7.0975	22.52	24.62	1.3434	15.12	17.13
aQZ	x	6.6951	-1.77	-1.40	8.1096	11.47	13.87	1.4374	9.17	11.33
a5Z	x	6.6445	-1.00	-0.63	8.7334	4.66	7.25	1.6157	-2.09	0.33
CBSII		6.5589	0.30	0.66	9.9159	-8.25	-5.31	1.6232	-2.56	-0.13
CBSI		6.5809	-0.04	0.33	10.0372	-9.58	-6.60	1.5897	-0.45	1.93
CBSII	x	6.5898	-0.17	0.19	9.5874	-4.67	-1.82	1.7616	-11.31	-8.67
CBSI	x	6.6149	-0.55	-0.19	9.0993	0.66	3.36	1.7211	-8.75	-6.17
CBSII*		6.5623	0.25	0.61	10.2478	-11.87	-8.84	1.7962	-13.50	-10.80
CBSI*		6.5800	-0.02	0.34	10.0441	-9.65	-6.67	1.5895	-0.43	1.95
CBSII*	x	6.6114	-0.50	-0.13	9.2306	-0.77	1.97	1.5958	-0.83	1.56
CBSI*	x	6.6177	-0.60	-0.23	9.1127	0.52	3.22	1.5925	-0.63	1.76
OW	NA	6.5785	0.00	0.36	9.1601	0.00	2.71	1.5826	0.00	2.37
HL	x	6.6026	-0.37	0.00	9.4157	-2.79	0.00	1.6210	-2.43	0.00

All values are in atomic units.

^a Abbreviation "HL" refers to the high-level calculations as described in the text; "OW" refers to the data of Ogilvie [83]. The columns $\Delta_{Property}^{Ref}$ are the relative signed difference (see text) of the property as compared with Ogilvie and the high-level calculations.

^b Abbreviation "x" denotes the use of counterpoise correction or the use of counterpoise corrected data in the CBS extrapolation. The use of counterpoise correction does not apply to the data of Ogilvie.

those derived from the extrapolated PESs. An interesting feature of these data is the effect of counterpoise correction. Consider the ω_e values resulting from the direct extrapolation of the property with and without counterpoise correction. The BSSE-tainted values produce extrapolations that are smaller than and closer to the reference values, whereas the counterpoise-corrected values are larger than the reference values. The trend is reversed when deriving the properties from the CBS-extrapolated PESs; the counterpoise-corrected values are smaller than the reference values, whereas the extrapolated, BSSE-tainted surfaces are larger.

Error Analysis of Extrapolation Processes

In this subsection, error statistics for the properties across the set of six rare-gas dimer pairs are presented (Tables VIII, IX, and X). Listed are the mean unsigned error (MUE), mean signed error (MSE), root-mean-square (RMS) error, relative unsigned error (Δ_{Rel}), and maximum unsigned error (Δ_{Max}) for each extrapolation type and procedure with and without counterpoise correction with re-

spect to the both the experimental and high level reference data. The column " $\times 10^x$ " denotes the power multiplied to the statistic within the row. Tables VIII, IX, and X are discussed in the following three subsections.

Error Analysis of R_e . In examining Table VIII, it is useful to note that the high-level reference R_e values are slightly larger than the experimental values, with the exception of HeNe, whose reference values are nearly identical. With that in mind, the MUE of the extrapolations using uncorrected values are larger when compared with the high-level reference potential as opposed to the experimental Ogilvie and Wang reference data. In contrast, the MUE of the counterpoise-corrected values are smaller when compared with the high-level reference potential as opposed to the Ogilvie and Wang reference data. For all extrapolations, the MSE is smaller with respect to the high-level reference data compared with the experimental reference data, with the exception of the uncorrected CBSII. One generally observes larger errors in the R_e values derived from the CBS-extrapolated PES than the directly extrap-

TABLE VII
Comparison of NeAr CCSD(T)/CBS extrapolated properties with high-level reference calculations and those of Ogilvie.

Basis ^a	CP ^b	R_e	$\Delta_{R_e}^{OW}$	$\Delta_{R_e}^{HL}$	$D_e \times 10^4$	$\Delta_{D_e}^{OW}$	$\Delta_{D_e}^{HL}$	$\omega_e \times 10^4$	$\Delta_{\omega_e}^{OW}$	$\Delta_{\omega_e}^{HL}$
aTZ		6.6510	-0.86	-0.71	2.2740	-6.24	-10.45	1.3195	-3.01	-5.90
aQZ		6.6164	-0.33	-0.19	2.2194	-3.69	-7.80	1.2275	4.17	1.49
a5Z		6.6038	-0.14	0.00	2.1716	-1.45	-5.48	1.2571	1.87	-0.88
aTZ	x	6.8350	-3.65	-3.50	1.3791	35.57	33.02	1.0497	18.05	15.76
aQZ	x	6.7066	-1.70	-1.56	1.7121	20.01	16.84	1.1273	12.00	9.54
a5Z	x	6.6508	-0.85	-0.71	1.8895	11.72	8.22	1.2644	1.30	-1.47
CBSII		6.5964	-0.03	0.11	2.0792	2.86	-0.99	1.2417	3.06	0.35
CBSI		6.5964	-0.03	0.11	2.1434	-0.14	-4.11	1.2750	0.47	-2.32
CBSII	x	6.6079	-0.20	-0.06	2.0916	2.28	-1.59	1.3807	-7.79	-10.81
CBSI	x	6.6182	-0.36	-0.22	1.9933	6.87	3.18	1.3453	-5.02	-7.97
CBSII*		6.5992	-0.07	0.07	2.1234	0.79	-3.14	1.3180	-2.89	-5.77
CBSI*		6.5970	-0.04	0.10	2.1437	-0.15	-4.12	1.2746	0.50	-2.29
CBSII*	x	6.6166	-0.33	-0.19	2.0260	5.35	1.60	1.2395	3.24	0.53
CBSI*	x	6.6223	-0.42	-0.28	1.9969	6.71	3.01	1.2430	2.97	0.25
OW	NA	6.5946	0.00	0.14	2.1404	0.00	-3.96	1.2810	0.00	-2.80
HL	x	6.6038	-0.14	0.00	2.0588	3.81	0.00	1.2461	2.72	0.00

All values are in atomic units.

^a Abbreviation "HL" refers to the high-level calculations as described in the text; "OW" refers to the data of Ogilvie [83]. The columns $\Delta_{property}^{Ref}$ are the relative signed difference (see text) of the property as compared with Ogilvie and the high-level calculations.

^b Abbreviation "x" denotes the use of counterpoise correction or the use of counterpoise corrected data in the CBS extrapolation. The use of counterpoise correction does not apply to the data of Ogilvie.

olated values. In comparison with the experimental reference data, the MUE and MSE for both uncorrected and counterpoise-corrected versions of CBSII** are significantly larger than those of CBSII, whereas CBSI and CBSI* shows very similar errors. It is interesting to note that the errors of CBSI and CBSI* increase when counterpoise-corrected data is used in the extrapolation process.

The CBS procedure/type that agrees most closely with the high-level reference data is the counterpoise-corrected CBSII, which is a direct extrapolation of counterpoise-corrected data. It exhibits the smallest MUE, the second smallest MSE, and third smallest RMS found on the table. In comparison with the experimental data, the error increases but is only marginally worse than the best statistics seen with the experimental reference.

Error Analysis of D_e . In examining Table IX, it is useful to note that the high-level reference D_e values are slightly smaller than the experimental ones. With the exceptions of CBSI and CBSI* in relation to the experimental reference, CBS values of D_e with counterpoise corrections have system-

atically lower errors with respect to the high-level reference data than the corresponding uncorrected counterparts. One generally observes smaller errors in the D_e values derived from the CBS-extrapolated PES than the directly extrapolated values.

The CBS procedure/type that agrees most closely with any reference (which, again, is the high-level reference) is the counterpoise-corrected CBSII*, which is the observed property on the counterpoise-corrected CBS-extrapolated PES.

Error Analysis of ω_e . In examining Table X, it is useful to note that there is no distinct trend between the difference of ω_e with respect to the experimental and high-level reference data. This is perhaps followed by a similar lack in consistency when comparing the MUEs of the CBS values in relation to experimental and high-level data. With the exception of the comparison between the uncorrected CBSII and CBSII*, one generally observes significantly smaller MUEs in the ω_e values derived from the CBS-extrapolated PES than the directly extrapolated values.

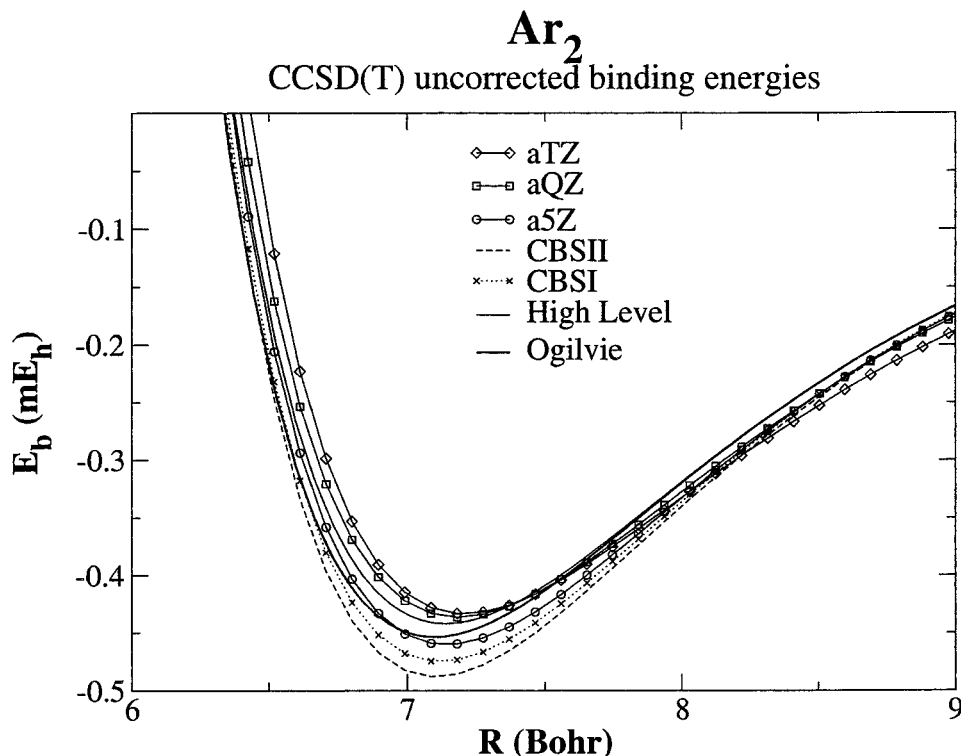


FIGURE 2. The Ar₂ binding energy PES as calculated without counterpoise correction at CCSD(T)/basis. “High Level” indicates the set of high-level reference data as explained in the text. “Ogilvie” refers to the potential as described in reference [42].

On the other hand, the MSE of counterpoise-corrected CBSII is an order of magnitude smaller than that of the counterpoise-corrected CBSII*. Similarly, the MSE of counterpoise-corrected CBSI is half that of counterpoise-corrected CBSI*.

The CBS procedure/type that agrees most with any reference data set (which happens to be the experimental reference) is the uncorrected CBSI*, which is the observed property on the CBS-extrapolated PES without counterpoise correction.

It is of interest to note that no particular procedure (direct extrapolation of property and extrapolation of the entire PES), type (CBSI and CBSII), or even counterpoise scheme (corrected and uncorrected) stands out as being best at obtaining all properties considered. In fact, a different combination of the above fundamental variables in the current study were found to compare best for with one of the reference data sets for each property.

APPLICATIONS OF THE MCCM-vdW MODEL

The past two sections have addressed the issue of deriving accurate, reliable results for PESs of van

der Waals systems, with special focus on the rare gases as prototype systems. In this subsection, focus is diverted toward new quantum models that allow highly accurate results to be obtained at a fraction of the computational cost (and human effort) of the methods previously discussed. To derive such models, extensive validation and testing is necessary, and, hence, the analysis of the previous sections remains an integral part.

Recently, a new MCCM was developed for the determination of accurate van der Waals PESs [27]. The method utilizes a novel parameterization strategy that simultaneously fits to very high-level binding, HF, and correlation energies of homonuclear and heteronuclear rare gas dimers of He, Ne, and Ar. The decomposition of the energy into HF and correlation components leads to a more reliable and transferable model. The main features of the model have been outlined above. Here, the model is further tested in the examination of three-body interactions of helium trimer and on the rare gas–water PESs. The latter is related to methods used to derive van der Waals parameters in molecular simulation force fields.

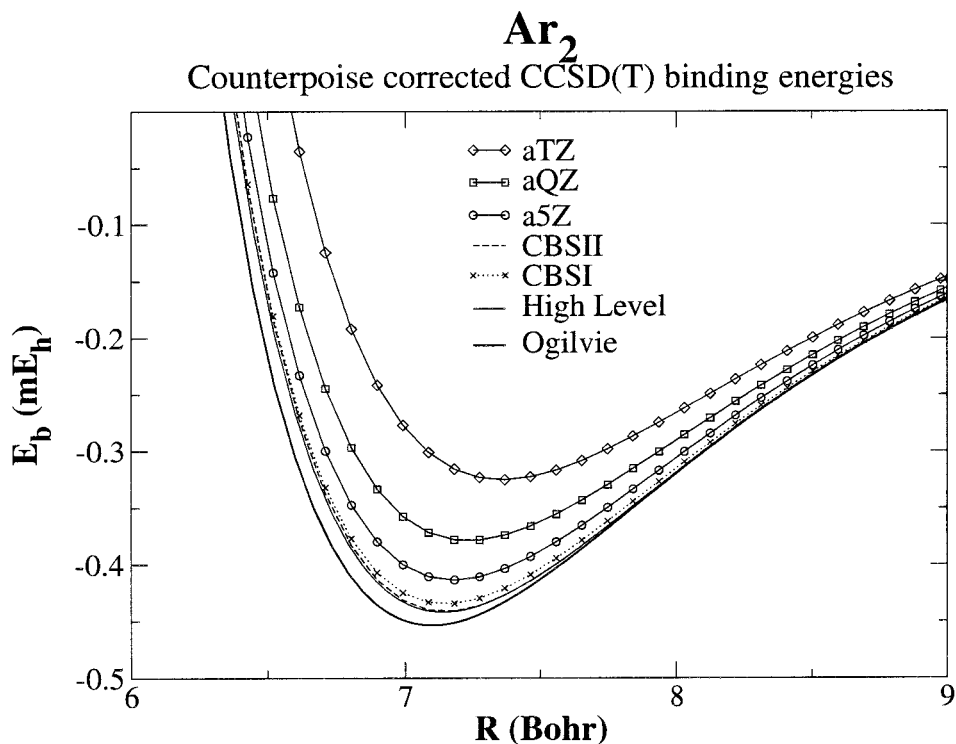


FIGURE 3. The Ar₂ binding energy PES as calculated with counterpoise correction at CCSD(T)/basis. “High Level” indicates the set of high-level reference data as explained in the text. “Ogilvie” is the potential as described in reference [42].

He₃

In this section, MCCM-vdW is applied to rare-gas trimers to demonstrate that model’s transfer-

ability beyond two-body systems and, in particular, to assess the ability of the model to reproduce accurate three-body energies. Use of the MCCM-vdW

TABLE VIII
Comparison of R_e difference statistics across all dimers between CBS methods with the experimental (OW) and high-level (HL) reference data.

Ref		$\times 10^x$	Uncorrected				Counterpoise corrected			
			CBSII	CBSII*	CBSI	CBSI*	CBSII	CBSII*	CBSI	CBSI*
OW	MUE	2	1.49	2.43	1.69	1.65	1.82	2.92	3.11	3.19
	MSE	2	0.44	1.16	1.69	1.65	1.57	2.92	3.11	3.19
	RMS	2	1.30	2.10	1.62	1.53	1.67	1.21	1.28	1.39
	Δ_{Rel}	2	0.32	0.51	0.37	0.36	0.39	0.50	0.54	0.56
	Δ_{Max}	2	3.60	6.01	4.36	4.08	4.76	4.91	5.20	5.08
HL	MUE	2	2.16	2.77	1.81	1.67	1.06	1.31	1.48	1.56
	MSE	2	-1.20	-0.47	0.06	0.02	-0.06	1.29	1.48	1.56
	RMS	2	2.08	1.57	0.85	0.80	0.63	1.05	0.31	0.54
	Δ_{Rel}	2	0.48	0.51	0.32	0.29	0.20	0.27	0.24	0.26
	Δ_{Max}	2	4.93	4.69	3.04	2.76	2.07	3.13	1.91	2.46

Listed are the MUE, MSE, RMS, Δ_{Rel} , and Δ_{Max} . All values are atomic units.

TABLE IX

Comparison of D_e difference statistics across all dimers between CBS methods with the experimental (OW) and high-level (HL) reference data.

Ref		$\times 10^x$	Uncorrected				Counterpoise corrected			
			CBSII	CBSII*	CBSI	CBSI*	CBSII	CBSII*	CBSI	CBSI*
OW	MUE	6	14.24	10.09	6.13	6.27	3.82	6.09	8.09	7.81
	MSE	6	-2.48	5.55	3.74	3.91	2.09	-5.85	-8.09	-7.81
	RMS	6	11.24	12.73	7.74	8.05	3.03	4.96	7.78	7.56
	Δ_{Rel}	2	8.35	7.47	4.54	4.70	2.24	3.61	5.17	5.00
	Δ_{Max}	6	27.93	34.56	20.55	21.35	8.13	12.28	19.58	18.90
HL	MUE	6	14.53	11.50	8.46	8.59	5.54	2.41	4.64	4.36
	MSE	6	0.97	9.00	7.19	7.36	5.54	-2.41	-4.64	-4.36
	RMS	6	15.21	17.35	12.07	12.39	5.85	1.48	2.47	2.24
	Δ_{Rel}	2	9.93	9.83	6.96	7.12	3.80	1.33	2.48	2.31
	Δ_{Max}	6	39.45	46.29	32.38	33.08	16.73	4.05	7.85	7.17

Listed are the MUE, MSE, RMS, Δ_{Rel} , and Δ_{Max} . All values are atomic units.

model may provide a means of much more efficiently generating databases from which many-body force fields can be parameterized and/or tested. The parameters of the MCCM-vdW model were derived from two-body binding, HF-SCF, and correlation potential energies.

The PES of He_3 is studied along the radial dimension of an equilateral triangle configuration. Each angle was held fixed at 60 degrees, and the interatomic trimer distances were scaled such that they corresponded, for comparison, to the interatomic dimer distances reported by Cybulski and Toczylowski [16].

The highest-level calculations that could be performed on the trimer systems were at the CCSD(T)/a5Z level without bond functions or counterpoise corrections. To obtain the best possible binding, HF-SCF, and correlation reference PES for rare-gas clusters, the following two-body corrected model is introduced below. The analytic forms of the two-body binding, HF-SCF, and correlation reference PES at counterpoise-corrected CCSD(T)/a5Z+(3s3p2d2f1g)bf levels for rare-gas homodimers and heterodimers involving He, Ne, and Ar were presented and discussed in detail elsewhere [16, 17]. These curves can be used to correct the two-body

TABLE X

Comparison of ω_e difference statistics across all dimers between CBS methods with the experimental (OW) and high-level (HL) reference data.

Ref		$\times 10^x$	Uncorrected				Counterpoise corrected			
			CBSII	CBSII*	CBSI	CBSI*	CBSII	CBSII*	CBSI	CBSI*
OW	MUE	6	9.76	13.13	7.27	5.85	9.04	5.31	10.41	6.65
	MSE	6	-7.11	7.29	-4.51	0.52	0.68	-4.65	-3.40	-6.30
	RMSD	6	9.98	8.60	5.70	6.26	6.35	5.33	6.16	6.20
	Δ_{Rel}	2	9.63	10.83	6.37	5.91	7.62	5.19	8.35	6.27
	Δ_{Max}	6	29.59	21.99	13.86	15.37	17.90	14.91	17.95	16.34
HL	MUE	6	7.97	12.61	7.47	6.79	10.25	5.03	11.62	6.68
	MSE	6	-7.49	6.91	-4.90	0.14	0.30	-5.03	-3.78	-6.68
	RMSD	6	12.78	6.94	5.80	0.53	5.04	4.39	5.57	6.01
	Δ_{Rel}	2	10.35	9.89	6.50	5.91	7.85	4.59	8.85	6.18
	Δ_{Max}	6	33.36	19.29	17.63	13.67	16.50	13.21	20.65	14.64

Listed are the MUE, MSE, RMS, Δ_{Rel} , and Δ_{Max} . All values are atomic units.

energy contributions for rare-gas clusters calculated with a cheaper level of theory (including the MCCM-vdW model, although the purpose here is to test the uncorrected MCCM-vdW model). The form of the very-high-level cluster energy model with two-body corrections, using the uncorrected theory level of CCSD(T)/a5Z, is given by

$$E^{VHL} = E^{CCSD(T)/a5Z} + \sum_{i<j} \Delta_{ij} \quad (14)$$

$$E^{VHL(X)} = E^{HF/a5Z} + \sum_{i<j} \Delta_{ij}^{(X)} \quad (15)$$

$$\begin{aligned} E^{VHL(C)} &= E^{VHL} - E^{VHL(X)} \\ &= E^{CCSD(T)/a5Z} - E^{HF/a5Z} + \sum_{i<j} \Delta_{ij}^{(C)}, \end{aligned} \quad (16)$$

where $E^{CCSD(T)/a5Z}$ and $E^{HF/a5Z}$ are the energies of the rare-gas cluster at the uncorrected level of theory and E^{VHL} , $E^{VHL(X)}$, and $E^{VHL(C)}$ are the corrected total, HF-SCF, and correlation energies of the clusters, respectively. The two-body correct terms are given by

$$\Delta_{ij} = E^{CCSD(T)/\text{ref}}(Rg_i : Rg_j) - E^{CCSD(T)/a5Z}(Rg_i : Rg_j), \quad (17)$$

$$\Delta_{ij}^{(X)} = E^{HF/\text{ref}}(Rg_i : Rg_j) - E^{HF/a5Z}(Rg_i : Rg_j), \quad (18)$$

$$\Delta_{ij}^{(C)} = \Delta_{ij} - \Delta_{ij}^{(X)}, \quad (19)$$

where the notation $(Rg_i : Rg_j)$ denotes the two-body interaction between rare-gas i and j in the cluster, obtained from a separate calculation or, in the current case, from analytic forms fitted very accurately to the two-body PES at each level of theory. These potential energy curves are available elsewhere [27].

The reference three-body binding, HF-SCF, and correlation energies (denoted as 3-body, 3-body(X), and 3-body(C), respectively) were calculated at the CCSD(T)a5Z level as

$$E_{3\text{-body}}^{a5Z} = E^{CCSD(T)/a5Z} - \sum_{i<j} E^{CCSD(T)/a5Z}(Rg_i : Rg_j), \quad (20)$$

$$E_{3\text{-body}(X)}^{a5Z} = E^{HF/a5Z} - \sum_{i<j} E^{HF/a5Z}(Rg_i : Rg_j), \quad (21)$$

$$E_{3\text{-body}(C)}^{a5Z} = E_{3\text{-body}}^{a5Z} - E_{3\text{-body}(X)}^{a5Z}. \quad (22)$$

Similarly, the MCCM-vdW three-body, three-body HF-SCF, and three-body correlation potential are defined as

$$E_{3\text{-body}}^{\text{MCCM-vdW}} = E^{\text{MCCM-vdW}} - \sum_{i<j} E^{\text{MCCM-vdW}}(Rg_i : Rg_j), \quad (23)$$

$$\begin{aligned} E_{3\text{-body}(X)}^{\text{MCCM-vdW}} &= E^{\text{MCCM-vdW}(X)} \\ &\quad - \sum_{i<j} E^{\text{MCCM-vdW}(X)}(Rg_i : Rg_j), \end{aligned} \quad (24)$$

$$\begin{aligned} E_{3\text{-body}(C)}^{\text{MCCM-vdW}} &= E^{\text{MCCM-vdW}(C)} \\ &\quad - \sum_{i<j} E^{\text{MCCM-vdW}(C)}(Rg_i : Rg_j). \end{aligned} \quad (25)$$

In general, the three-body energies (Fig. 4) are small relative to the corresponding two-body energies. At small interatomic distances (in the repulsive region of the binding energy), the three-body energies become larger. The three-body contribution to the binding energy is generally attractive except in the region of the minimum, where it is observed to be very slightly repulsive. The three-body HF-SCF and correlation energies are attractive and repulsive, respectively.

The MCCM-vdW model is able to closely reproduce the total binding energy and three-body PESs for both the exchange (X) and correlation (C) components (Fig. 4). This is an encouraging result, because only two-body interactions were used to parameterize the MCCM-vdW model.

He ··· H₂O

In this subsection, the transferability of the MCCM-vdW model is explored in the interaction of helium with water. This is an important problem not only from a fundamental chemical physics point of view but also from the perspective of the design of transferable molecular simulation force fields, where rare gases are often used as probes to derive nonbonded van der Waals parameters [84–86].

A high-level reference PESs for helium–water was generated at the CCSD(T)/a5Z level of theory with a supplementary set of (3s3p2d) bond functions [87] and counterpoise corrections. The O–H bond lengths were held fixed at 0.957 Å and the H–O–H bond angle was held fixed at 104.5 degrees. The coordinate varied was the radial distance (2.50,

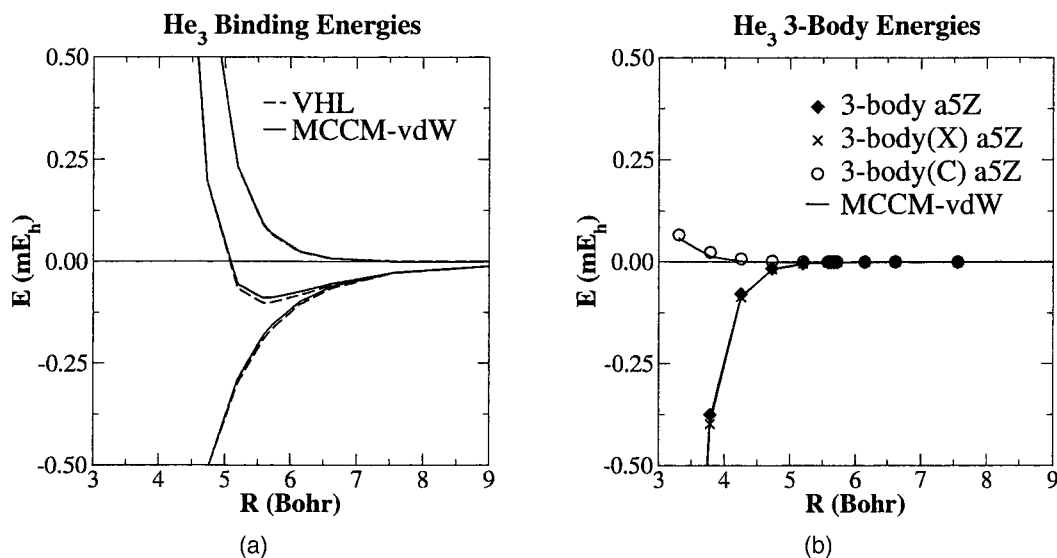


FIGURE 4. Comparison of the D_{3h} “breathing” coordinate of the He_3 trimer PES between available quantum data and MCCM-vdW. (a) Binding energy as compared with the “very-high-level” data (VHL, see text) and MCCM-vdW. The HF-SCF and post-SCF (correlation) components are also shown. (b) Comparison of the three-body portion of the binding energy between CCSD(T)/a5Z and MCCM-vdW. Again, the energy is broken into HF-SCF (3-body(X)/a5Z) and correlation (3-body(C)/a5Z) components.

2.75, 3.00, 3.25, 3.50, 3.75, 4.00, 4.25, 4.50, and 5.00 Å) between the center of mass of the water and helium along the C_{2v} axis of the water in the direction of the oxygen.

In addition, a protocol used for molecular simulation force field design [MP3/6-311++G(3d,3p)] [84–86] was employed for comparison. The MP3 protocol has been used to probe molecules with rare gases to obtain the Lennard–Jones nonbonded interaction potential parameters used in molecular mechanics calculations and molecular simulations. Figure 5 displays the binding energy of $\text{He} \cdots \text{H}_2\text{O}$ as determined from MP3/6-311++G(3d,3p), MCCM-vdW, and CCSD(T)/a5Z(3s3p2d) with counterpoise correction (referred to as “reference”). In addition, Figure 5 displays the energy decomposition of the MCCM-vdW and reference potentials into HF-SCF and correlation potential energy components.

The observed slight underbinding predicted by the MCCM-vdW model for the $\text{He} \cdots \text{H}_2\text{O}$ system is likely related to the very weak He interactions that are notoriously difficult to capture quantum mechanically [36, 46–56]. The MP3/6-311++G(3d,3p) protocol, which is a computationally cheaper method, does not agree as well with the high-level calculations.

The inclusion of attractive dispersive forces in force fields and semiempirical methods is of great

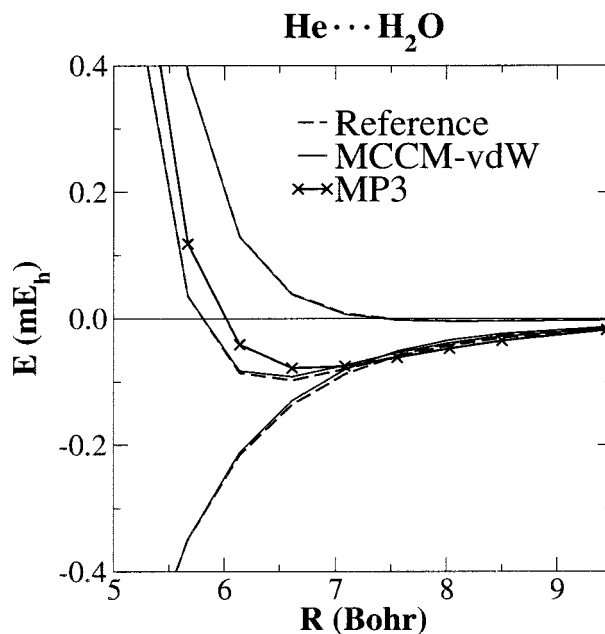


FIGURE 5. Comparison of methods for the C_{2v} radial portion of the $\text{He} \cdots \text{H}_2\text{O}$ (fixed experimental monomer geometry) PES. The radial axis measures the separation of the monomer’s center of mass. “Reference” refers to counterpoise-corrected CCSD(T)/a5Z supplemented with a set of 3s3p2d bond functions; MCCM-vdW, the multilevel method discussed in the text; MP3, MP3/6-311++G(3d,3p). The reference and MCCM-vdW methods are additionally broken down into HF-SCF and post-HF components.

importance [11]. Recently, effort was made to include modified pairwise core-core interactions based on ab initio PESs to improve the description of hydrogen-bonded systems [88, 89]. The creation of pairwise correlation potential is of significant interest for the development of new semiempirical methods. One must, however, have a method for obtaining accurate correlation potentials in order to fully explore the idea. The development of the MCCM-vdW model that can reliably reproduce binding, HF-SCF, and correlation energies involving rare gases is therefore of considerable interest.

Conclusion

In the current paper, rare-gas dimer PESs and related quantities are calculated using state-of-the-art ab initio methods and compared with experimental values, including second virial coefficients. With exception to the small temperature regime of light dimers, the classical second virial coefficients obtained from ab initio potentials agree closely with experimental values but are generally too large when compared with experiment for most temperatures. The quantum-corrected values are slightly too large of all dimers at all temperatures. This arises from a slight underbinding of the dimers predicted at this level of theory.

In addition, several procedures for performing CBS extrapolations are discussed and compared. Comparison is made between direct CBS extrapolation of the properties versus derivation from the CBS extrapolated PES itself. Different functional forms of the CBS extrapolation were tested using both uncorrected and counterpoise-corrected data. Different procedures were observed to sometimes result in significantly different results. No extrapolation type/procedure was found to be clearly superior upon comparison with the reference data.

A MCCM for the determination of PESs for van der Waals interactions (MCCM-vdW) was discussed, and results for helium trimers and helium-water interactions were presented. The model, which was parameterized only to rare-gas dimer data, was observed to closely reproduce the binding energy, including two-body and three-body exchange and correlation components. Application of the model to the helium-water PES was also examined. The MCCM-vdW model was able to very closely reproduce high-level ab initio results for a fraction of the computational cost. Of very promising note is the ability of MCCM-vdW to reproduce

interaction energies of molecules that contain atoms not within the parameterization set.

It is hoped that the data presented here represent a step toward the design of new semiempirical and empirical force fields for molecular simulations.

ACKNOWLEDGMENT

One of the authors (D. Y.) is grateful for financial support provided by the National Institutes of Health (grant number 1R01-GM62248-01A1) and the Donors of The Petroleum Research Fund, administered by the American Chemical Society. One of the authors (T. G.) was partially supported by a fellowship from the Chemical Physics program at the University of Minnesota and from a National Institutes of Health Molecular Biophysics Training Grant. Computational resources were provided by the Minnesota Supercomputing Institute.

References

1. Head-Gordon, M. *J Phys Chem* 1996, 100, 13213–13225.
2. Liu, Y.-P.; Kim, K.; Berne, B. J.; Friesner, R. A.; Rick, S. W. *J Chem Phys* 1998, 108, 4739–4755.
3. Foloppe, N.; MacKerell, A. D., Jr. *J Comput Chem* 2000, 21, 86–104.
4. Halgren, T. A.; Damm, W. Polarizable force fields. *Curr Opin Struct Biol* 2001, 11, 236–242.
5. Wang, W.; Donini, O.; Reyes, C. M.; Kollman, P. A. *Annu Rev Biophys Biomol Struct* 2001, 30, 211–243.
6. Chen, B.; Xing, J.; Siepmann, J. I. *J Phys Chem B* 2000, 104, 2391–2401.
7. Wick, C. D.; Martin, M. G.; Siepmann, J. I. *J Phys Chem B* 2000, 104, 8008–8016.
8. Gao, J.; Truhlar, D. G. *Annu Rev Phys Chem* 2002, 53, 467–505.
9. Warshel, A. *Acc Chem Res* 2002, 35, 385–395.
10. Merz, K. M., Jr.; Stanton, R. V. In *Encyclopedia of Computational Chemistry*; Schleyer, P.; Allinger, N.; Clark, T.; Gasteiger, J.; Kollman, P.; Schaefer, H., III; Schreiner, P., Eds., Vol. 2; John Wiley & Sons: Chichester, 1998; p 2330–2343.
11. Thiel, W. In *Perspectives on Semiempirical Molecular Orbital Theory*; Adv. Chem. Phys.; Prigogine, I.; Rice, S. A., Eds., Vol. 93; John Wiley & Sons: New York, 1996; p 703–757.
12. Chałasiński, G.; Szczęśniak, M. M. *Chem Rev* 1994, 94(7), 1723–1765.
13. Chałasiński, G.; Szczęśniak, M. M. *Chem Rev* 2000, 100, 4227–4252.
14. Dunning, T. H., Jr. *J Chem Phys* 1989, 90, 1007–1023.
15. Woon, D. E.; Dunning, T. H., Jr. *J Chem Phys* 1994, 100, 2975–2988.
16. Cybulski, S. M.; Toczyłowski, R. R. *J Chem Phys* 1999, 111, 10520–10528.

17. Giese, T. J.; Audette, V. M.; York, D. M. *J Chem Phys* 2003, 119, 2618–2622.
18. Boys, S. F.; Bernardi, F. *Mol Phys* 1970, 19(4), 553–566.
19. MOLPRO is a package of ab initio programs written by H.-J. Werner and P. J. Knowles, with contributions from R. D. Amos, A. Bernhardsson, A. Berning, P. Celani, D. L. Cooper, M. J. O. Deegan, A. J. Dobyn, F. Eckert, C. Hampel, G. Hetzer, T. Korona, R. Lindh, A. W. Lloyd, S. J. McNicholas, F. R. Manby, W. Meyer, M. E. Mura, A. Nicklass, P. Palmieri, R. Pitzer, G. Rauhut, M. Schütz, H. Stoll, A. J. Stone, R. Tarroni, and T. Thorsteinsson.
20. Wood, D. E.; Dunning, T. H., Jr. *J Chem Phys* 1993, 99(3), 1914–1929.
21. Woon, D. E.; Dunning, T. H., Jr. *J Chem Phys* 1994, 101(10), 8877–8893.
22. Peterson, K. A.; Woon, D. E.; Dunning, T. H. Jr. *J Chem Phys* 1994, 100, 7410–7415.
23. Feller, D. *J Chem Phys* 1992, 96(8), 6104–6114.
24. Feller, D. *J Chem Phys* 1993, 98(9), 7059–7071.
25. Feller, D.; Peterson, K. A. *J Chem Phys* 1998, 108, 154–176.
26. van Mourik, T.; Wilson, A. K.; Peterson, K. A.; Woon, D. E.; Dunning, T. H., Jr. *Adv Quantum Chem* 1998, 31, 105–135.
27. Giese, T. J.; York, D. M. *J Chem Phys* 2004, 120, 590–602.
28. Burda, J. V.; Zahradník, R.; Hobza, P.; Urban, M. *Mol Phys* 1996, 89(2), 425–432.
29. Zhang, Y.; Pan, W.; Yang, W. *J Chem Phys* 1997, 107, 7921–7925.
30. Patton, D. C.; Pederson, M. R. *Int J Quantum Chem* 1998, 69, 619–627.
31. González-Lezana, T.; Rubayo-Soneira, J.; Miret-Artés, S.; Gianturco, F.; Delgado-Barrio, G.; Villarreal, P. *J Chem Phys* 1999, 110, 9000–9010.
32. Pérez-Jordá, J. M.; San-Fabián, E.; Pérez-Jiménez, A. J. *J Chem Phys* 1999, 110(4), 1916–1920.
33. van Mourik, T.; Wilson, A. K.; Dunning, T. H., Jr. *Mol Phys* 1999, 96(4), 529–547.
34. Maroulis, G. *J Phys Chem A* 2000, 104, 4772–4779.
35. Chałasiński, G.; Gutowski, M. *Chem Rev* 1988, 88(6), 943–962.
36. Bukowski, R.; Jeziorski, B.; Szalewicz, K. *J Chem Phys* 1996, 104(9), 3306–3319.
37. Dunning, T. H., Jr.; Peterson, K. A.; Wilson, A. K. *J Chem Phys* 2001, 114(21), 9244–9253.
38. Tao, F.-M. *J Chem Phys* 1993, 98, 3049–3059.
39. Tao, F.-M. *J Chem Phys* 1999, 111, 2407–2413.
40. Tao, F.-M.; Pan, Y.-K. *J Chem Phys* 1992, 97, 4989–4995.
41. van Duijneveldt, F. B.; van Duijneveldt-van de Rijdt, J.; van Lenthe, J. H. *Chem Rev* 1994, 94(7), 1873–1885.
42. Ogilvie, J. F.; Wang, F. Y. *J Mol Struct* 1992, 273, 277–290.
43. Ogilvie, J.; Wang, F. Y. *J Mol Struct* 1993, 291, 313–322.
44. McQuarrie, D. A. *Statistical Mechanics*. University Science Books: Mill Valley, 1973.
45. Kestin, J. K.; Knierim, E. A. M.; Najafi, B.; Ro, S. T.; Waldman, M. *J Phys Chem Ref Data* 1984, 13(1), 229–238.
46. Anderson, J. B.; Traynor, C. A.; Boghosian, B. M. *J Chem Phys* 1993, 99(1), 345–351.
47. Janzen, A. R.; Aziz, R. A. *J Chem Phys* 1997, 107, 914–919.
48. Aziz, R. A.; Slaman, M. J. *J Chem Phys* 1991, 94(12), 8047–8053.
49. Gdanitz, R. J. *J Chem Phys* 2000, 113, 5145–5153.
50. Klopper, W.; Noga, J. *J Chem Phys* 1995, 103(14), 6127–6132.
51. Klopper, W. *J Chem Phys* 2001, 115(2), 761–765.
52. Korona, T.; Williams, H. L.; Bukowski, R.; Jeziorski, B.; Szalewicz, K. *J Chem Phys* 1997, 106(12), 5109–5122.
53. Tang, K. T.; Toennies, J. P.; Yiu, C. L. *Phys Rev Lett* 1995, 74, 1546–1549.
54. van Mourik, T.; Dunning, T. H., Jr. *J Chem Phys* 1999, 111, 9248–9258.
55. Tang, K. T.; Toennies, J. P. *J Chem Phys* 2003, 118(11), 4976–4983.
56. Jeziorska, M.; Bukowski, R.; Cencek, W.; Jaszunski, M.; Jeziorski, B.; Szalewicz, K. *Collection Czech Chem Comm* 2003, 68(3), 463–488.
57. McLure, I. A.; Ramos, J. E.; Del Río, F. *J Phys Chem B* 1999, 103, 7019–7030.
58. Feller, D.; Peterson, K. *J Mol Struct (THEOCHEM)* 1997, 400, 69–92.
59. van Mourik, T.; Dunning, T. H., Jr. *J Chem Phys* 1997, 107(7), 2451–2462.
60. Woon, D. E. *Chem Phys Lett* 1993, 204(1–2), 29–35.
61. Woon, D. E.; Dunning, T. H., Jr. *J Chem Phys* 1995, 103, 4572–4585.
62. Peterson, K. A.; Dunning, T. H., Jr. *J Chem Phys* 1995, 102(5), 2032–2041.
63. Peterson, K.; Dunning, T., Jr. *J Phys Chem* 1995, 99, 3898–3901.
64. Masamura, M. *Theor Chem Acc* 2001, 106, 301–313.
65. Ochterski, J. W.; Petersson, G. A.; Montgomery, J. A., Jr. *J Chem Phys* 1996, 104(7), 2598–2619.
66. Martin, J.; Taylor, P. *Chem Phys Lett* 1996, 248, 336–344.
67. Shin Lee, J.; Yong Park, S. *J Chem Phys* 2000, 112(24), 10746–10753.
68. Hinde, R. *J Phys Chem A* 2000, 104, 7580–7585.
69. Peterson, K. A.; Wilson, A. K.; Woon, D. E.; Dunning, T. H., Jr. *Theor Chem Acc* 1997, 97, 251–259.
70. Xantheas, S. S. *J Chem Phys* 1996, 104(21), 8821–8824.
71. Toth, A. M.; Liptak, M. D.; Phillips, D. L.; Shields, G. C. *J Chem Phys* 2001, 114(10), 4595–4606.
72. Ramakrishna, V.; Duke, B. J. *J Chem Phys* 2003, 118(14), 6137–6143.
73. Montgomery, J. A., Jr.; Frisch, M. J.; Ochterski, J. W.; Petersson, G. A. *J Chem Phys* 2000, 112, 6532–6542.
74. Petersson, G. A.; Al-Laham, M. A. *J Chem Phys* 1991, 94(9), 6081–6090.
75. Woon, D. E.; Peterson, K. A.; Dunning, T. H., Jr. *J Chem Phys* 1998, 109, 2233–2241.
76. He, Y.; Cremer, D. *J Phys Chem A* 2000, 104, 7679–7688.
77. Cremer, D.; Kraka, E.; He, Y. *J Mol Struct* 2001, 567–568, 275–293.
78. Martin, J. *Chem Phys Lett* 1996, 259, 669–678.
79. Curtiss, L. A.; Raghavachari, K.; Redfern, P. C.; Stefanov, B. B. *J Chem Phys* 1998, 108(2), 692–697.

GIESE AND YORK

80. Paizs, B.; Salvador, P.; Császár, A.; Duran, M.; Suhai, S. *J Comput Chem* 2001, 22(2), 196–207.
81. Patel, K.; Butler, P. R.; Ellis, A. M.; Wheeler, M. D. *J Chem Phys* 2003, 119(2), 909–919.
82. Feller, D.; Sordo, J. A. *J Chem Phys* 2000, 113(2), 485–493.
83. Ogilvie, J. F.; Wang, F. Y. H. *J Mol Struct* 1993, 29, 313–322.
84. Yin, D.; MacKerell, A. D., Jr. *J Phys Chem* 1996, 100(7), 2588–2596.
85. Yin, D.; MacKerell, A. D., Jr. *J Comput Chem* 1998, 19(3), 334–348.
86. Jen Chen, I.; Daxu Yin, A. D. M. *J Comput Chem* 2002, 23(2), 199–213.
87. Tao, F.; Klemperer, W. *J Chem Phys* 1994, 101(2), 1129–1145.
88. Bernal-Uruchurtu, M.; Ruiz-López, M. *Chem Phys Lett* 2000, 330, 118–124.
89. Bernal-Uruchurtu, M. I.; Martins-Costa, M. T. C.; Millot, C.; M. F. R.-L. *J Comput Chem* 2000, 21, 572–581.
90. Fernandez, B.; Hattig, C.; Koch, H.; Rizzo, A. *J Chem Phys* 1999, 110, 2872–2882.
91. Koch, H.; Hattig, C.; Larsen, H.; Olsen, J.; Jorgensen, P.; Fernandez, B.; Rizzo, A. *J Chem Phys* 1999, 111, 10108–10118.
92. Hattig, C.; Larsen, H.; Olsen, J.; Jorgensen, P.; Koch, H.; Fernandez, B.; Rizzo, A. *J Chem Phys* 1999, 111, 10099–10107.